Journal of Polymer Science

WILEY

JOURNAL OF POLYMER SCIENCE

RESEARCH ARTICLE OPEN ACCESS

The Role of Residual Hydrogen Peroxide for Biological Applications of Polymeric *N*-Oxides

Michelle Kobus[1] | Shirin Mesgarha[1] | Erica Moretto[1] | Jon Wullenweber[2,3] | Mathias Ernst[2,3] | Sebastian G. Wicha[1] | Wolfgang Maison[1]

[1]Universität Hamburg, Institute of Pharmacy, Department of Chemistry, Hamburg, Germany | [2]Institute for Water Resources and Water Supply (B-11), Hamburg University of Technology, Hamburg, Germany | [3]DVGW Research Centre TUHH, Hamburg, Germany

Correspondence: Wolfgang Maison (wolfgang.maison@uni-hamburg.de)

Received: 11 July 2025 | **Revised:** 8 October 2025 | **Accepted:** 9 October 2025

Funding: This work was financial support from the Open Access Publication Fund of Universität Hamburg. This project has received funding from the Federal Ministry for Economic Affairs and Climate Action under the programme ZIM (Zentrales Innovationsprogramm Mittelstand) under grant agreement No KK5559001IE3.

Keywords: antifouling | biocides | *N*-oxides | polymer brushes | zwitterions

ABSTRACT

Polymers with *N*-oxide groups find applications in the biomedical field because they are highly hydrated in water, are considered to be nontoxic, and have stealth properties. Additional antimicrobial activity of polymeric *N*-oxides has also been reported, and it is currently unclear if this activity is a general feature of polymeric *N*-oxides or a special property of selected derivatives. *N*-Oxides are often prepared by oxidation of tertiary amines with hydrogen peroxide, which is notoriously difficult to remove from the resulting polymeric *N*-oxides. This study analyzes the role of residual oxidant in polymeric *N*-oxides for antimicrobial activity. Sensitive quantification reveals a significant release of hydrogen peroxide from oxidized polymers in solution and grafted on polyethylene or polyamide. The release of hydrogen peroxide from these polymers can lead to concentrations exceeding the minimum inhibitory concentrations (MICs) for *Staphylococcus aureus* and *Escherichia coli*. It can thus compromise microbiological assays. Rigorous removal of hydrogen peroxide leads to polymeric *N*-oxides with no antibacterial activity. Antibacterial effects of polymeric *N*-oxides against planktonic bacteria are primarily attributed to residual hydrogen peroxide, rather than to the intrinsic activity of the *N*-oxide functionality. Poly(*N*-oxide)-modified surfaces are therefore inert low-fouling materials with tunable, transient antibacterial functionality through controlled hydrogen peroxide release.

1 | Introduction

1.1 | *N*-Oxides

A class of compounds derived from the oxidation of tertiary aliphatic and aromatic aminesis characterized by a dative $N^+—O^-$ bond [1]. First identified in the early 20th century, *N*-oxides have attracted considerable attention due to their special chemical and physical properties. They have found widespread applications, for example, as oxidants in organic synthesis, hypoxia-activated drugs, targeting and release agents in nanomedicine, hydrophilic conjugates for drugs, antifouling materials, and conductive layers for optoelectronics [2].

Early studies focused largely on small-molecules. However, recent research has focused on applications of macromolecular *N*-oxides [3]. Polymeric *N*-oxides have excellent antifouling properties independent of the salt concentration of the surrounding media [4, 5] which has been demonstrated to prevent the adhesion of proteins and cells [6–8]. Their excellent blood compatibility and non-immunogenic properties make poly(*N*-oxides) promising alternatives to other zwitterionic

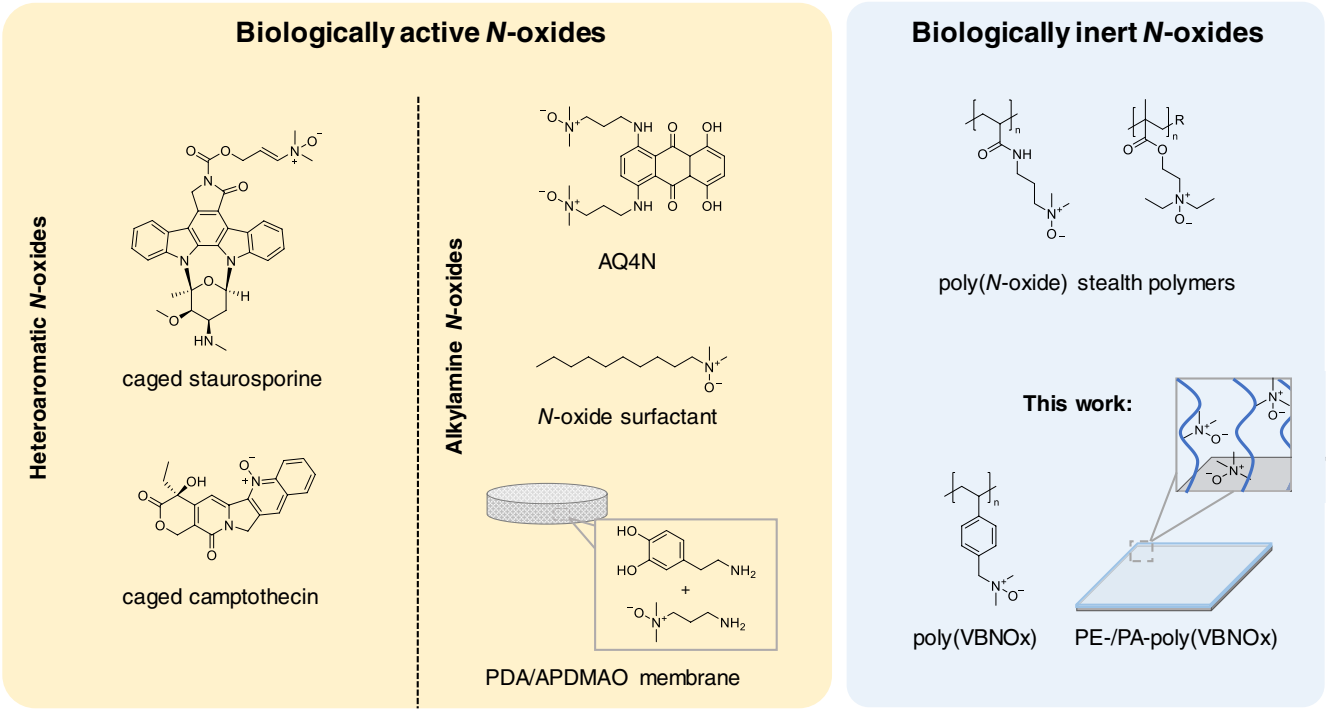

FIGURE 1 | Chemical structure drawings of heteroaromatic and alkylamine *N*-oxides. The compounds are categorized as biologically active or inert according to literature data.

polymers or polyethylene glycol in biomedical applications [2]. A key property of these polymers is their "stealth" characteristic, which allows them to effectively evade detection by the biological system [6]. For example, the conjugation of polyacrylamide-derived *N*-oxides to uricase has shown to improve solubility, increase blood half-life, and decrease immunogenicity of the protein in a mouse model [8]. Poly(*N*-oxides) also facilitate oral drug delivery by penetrating mucus layers and can enhance the efficacy of drug-loaded micelles used in chemotherapy [9]. These applications are based on the assumption that the *N*-oxide groups are inert under physiological conditions. At the same time, it is known that many *N*-oxides are chemically reactive, which is expressed, for example, in the field of organic synthesis through oxidation reactions or rearrangements [10, 11].

Some *N*-oxides of low molecular weight also have significant reactivity in biological systems, enabling their use as cytotoxic or antibacterial agents. The underlying bio-reductive mechanisms are well understood for some redox-reactive heteroaromatic *N*-oxides [12–15], but unclear for several alkylamine *N*-oxides (Figure 1) [12, 16]. Heteroaromatic compounds derived from staurosporine and camptothecin undergo reductive activation in the hypoxic tumor environment, leading to tumor-selective cytotoxicity [17, 18]. Notably, redox-responsive behavior is not limited to heteroaromatic *N*-oxides. For instance, AQ4N, an aliphatic *N*-oxide prodrug, undergoes bio-reduction to a potent topoisomerase II inhibitor, making it a strong candidate for tumor-targeted chemotherapy [15]. Similarly, long-chain alkylamine *N*-oxides have antimicrobial activity. However, the extent to which this activity is driven by their amphiphilic structure or other biochemical mechanisms is unclear [19–21].

For polymeric *N*-oxides, both stealth effects and antimicrobial activity have been described for very similar polymers. It is therefore difficult to determine which class of *N*-oxide a particular derivative belongs to (biologically reactive or inert). While poly(methacrylamide-*N*-oxide) showed no activity against *Streptococcus mutans* [22], other materials such as poly(*N*-oxide)-modified polyethylene (PE) demonstrated antibacterial effects against *Staphylococcus aureus* and *Escherichia coli* [23]. Furthermore, Zhang et al. demonstrated that modifying polydopamine membranes with alkylamine *N*-oxide moieties (PDA/APDMAO membrane) enhances antibacterial activity against *S. aureus* significantly, though the underlying mechanism remains unknown [24]. These conflicting findings further highlight the fundamental duality of *N*-oxides: some are unreactive and biologically inert (stealth properties), while others are chemically reactive agents that trigger specific biological responses (e.g., cytotoxicity or antibacterial activity).

Given the inconclusive results on the bioactivity of polymeric alkylamine *N*-oxides in previous studies, this work aims to explore the antibacterial and stealth properties of these compounds. The study addresses three key questions: (1) Does the redox activity of polymeric *N*-oxides cause antibacterial activity? (2) What is the influence of their charge state on antibacterial activity? and (3) how does oxidant contamination affect their antibacterial activity?

2 | Results and Discussion

Poly[(4-vinylbenzyl)-*N*,*N*-dimethylamine *N*-oxide] (poly(VBNOx)) was selected as a model compound for this study. Unlike

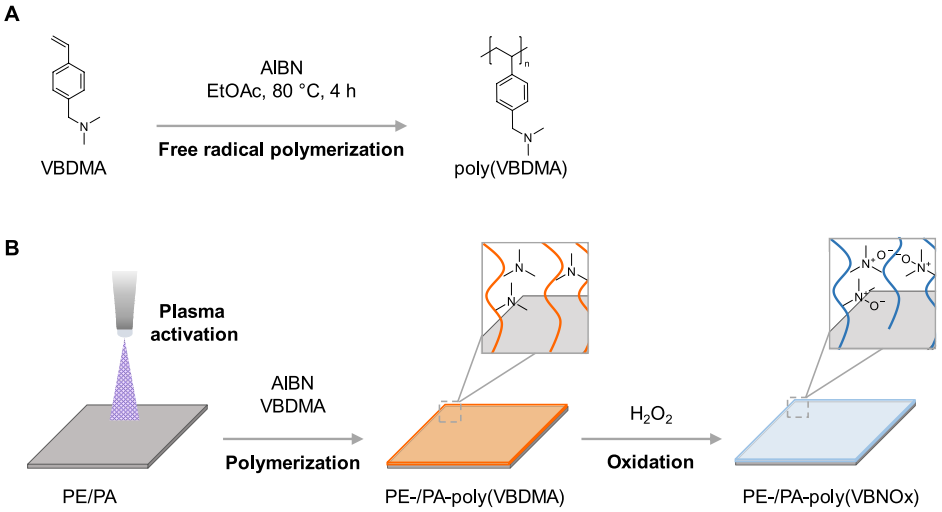

FIGURE 2 | (A) Free radical polymerization of (4-vinylbenzyl)-*N*,*N*-dimethylamine (VBDMA) with azobisisobutyronitrile (AIBN) for the preparation of poly(VBDMA), (B) Free radical graft polymerization of VBDMA from plasma-activated polyethylene (PE) and polyamide 6 (PA) for the preparation of PE-poly(VBDMA) and PA-poly(VBDMA), followed by oxidation with hydrogen peroxide to yield PE-poly(VBNOx) and PA-poly(VBNOx).

other polymeric *N*-oxides, such as polymethacrylate derivatives, poly(VBNOx) lacks β-hydrogen atoms or potentially reactive functionalities and is therefore not prone to elimination reactions or hydrolytic cleavage. It does not have any additional functional groups contributing to the charge of the polymer [23, 25, 26]. These structural features make it an ideal candidate for isolating the impact of the *N*-oxide moiety on antibacterial activity. In addition, poly(VBNOx) can be grafted easily from PE, and the resulting brush layers have been evaluated for their antifouling properties before [23].

The polymer was synthesized according to a known protocol in solution (Figure 2A). Briefly, poly(VBDMA) was prepared by polymerization of (4-vinylbenzyl)-*N*,*N*-dimethylamine (VBDMA), followed by oxidation with hydrogen peroxide to give poly(VBNOx) [27]. The oxidation of poly(VBDMA) to poly(VBNOx) was followed by NMR (Figure S1). The characteristic shift of the methylene and methyl groups adjacent to nitrogen allows the differentiation of poly(VBDMA) and poly(VBNOx). The analysis revealed that the oxidative conversion is almost complete after 48 h, and only a minor amount of residual amino groups (<2%) can be detected in the final oxidation product. A similar protocol was used for the synthesis of poly(VBNOx) brushes grafted from PE and polyamide 6 (PA) (Figure 2B). After plasma activation of the plastic surface, poly(VBDMA) brushes were prepared by free radical polymerization of VBDMA, followed by oxidation with hydrogen peroxide to give PE-poly(VBNOx) and PA-poly(VBNOx).

The redox activity of several drugs containing *N*-oxide groups is the reason for their biological activity. These drugs are activated under reductive conditions in vivo, leading to the generation of reactive oxygen species (ROS) [28]. ROS formation might thus also be the reason for the previously observed antibacterial effects of polymeric *N*-oxides. To determine whether the *N*-oxide groups in poly(VBNOx) contribute to ROS generation, a quantitative assay using the radical trapping agent 1,3-diphenylisobenzofuran (DPBF) was performed. DPBF reacts with various ROS species and allows their quantitative analysis by monitoring the decrease in absorption at 410 nm [29]. Briefly, poly(VBNOx) ($c = 8.3$ M) was incubated with DPBF ($c = 75\,\mu$M) for 24 h in the dark at 37°C. In contrast to previous experiments with similar ROS-trapping reagents [23], no significant ROS formation was detected under these conditions (Figure 3A,B).

An EPR spectroscopic evaluation of an aqueous poly(VBNOx) solution with 5,5-dimethyl-1-pyrroline *N*-oxide (DMPO) revealed also no signals, and confirmed the absence of radical species. As a highly sensitive detection method, spin-trap EPR spectroscopy can identify even low levels of ROS and indirectly detect short-lived radicals [30]. In contrast to earlier studies on poly(VBNOx) and similar polymers with *N*-oxide groups [31, 32], no radical species were detected at 37°C in MeOH. The formation of ROS is therefore most likely not the reason for antibacterial effects of polymeric *N*-oxides. However, an enzymatic (bio-reductive) activation of poly(VBNOx) in the presence of microorganisms cannot be excluded at this stage.

Many *N*-oxides are prepared by the oxidation of tertiary amines [23, 33]. These reactions are often slow, which can lead to the presence of unreacted amino groups in the resulting polymers. Protonation at physiological pH thus leads to the formation of positively charged structures with potential antimicrobial properties in solution and also upon contact of microorganisms with polymers on surfaces (contact biocidal activity) [34]. Almost complete oxidation of the polymer in solution (>98%) was confirmed via NMR spectroscopy (vide supra and Figure S1). However, for surface-grafted polymer brushes, the efficacy of oxidation might be decreased due to increased steric hindrance and limited reagent accessibility.

In light of these considerations, the oxidation of poly(VBDMA) brushes on a PE surface was examined. PE-poly(VBDMA) was prepared according to the method of Burmeister et al. and subsequently oxidized with hydrogen peroxide for 3 days to obtain PE-poly(VBNOx) [23]. The resulting material has been characterized by goniometry, x-ray photoelectron spectroscopy, time-of-flight secondary ion mass spectrometry, and IR spectroscopy

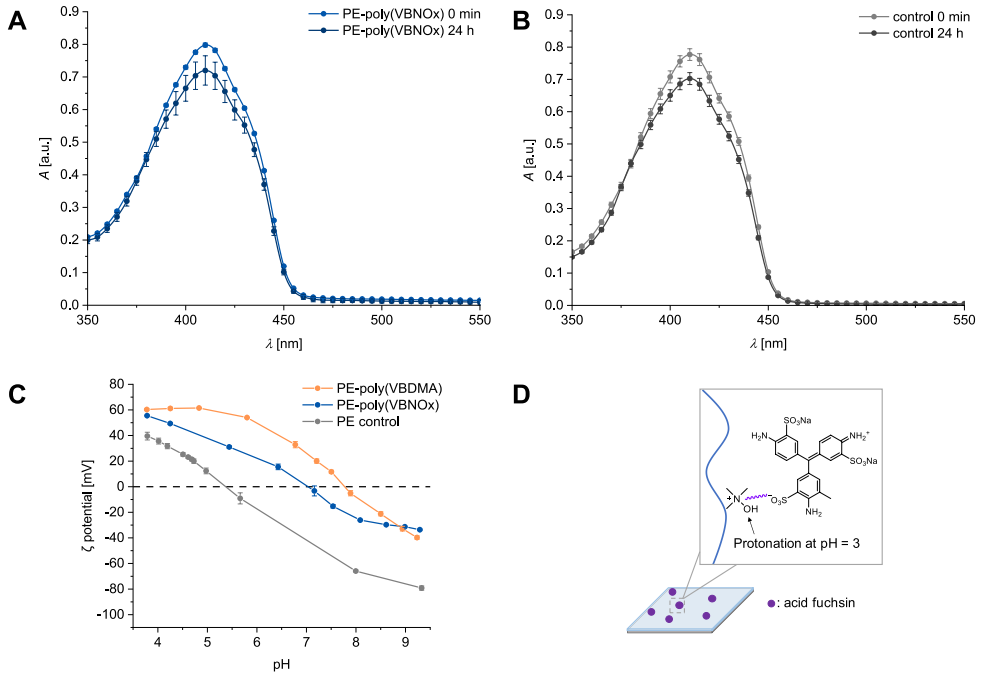

FIGURE 3 | (A) DPBF absorption spectra from 350 to 550 nm of $c(\text{DPBF})_{\text{start}} = 75\,\mu\text{M}$ in EtOH/MeOH (1:1) at $t = 0$ min and $t = 24$ h for the evaluation of potential ROS formation with addition of poly(VBNOx) with $c(N\text{-oxide}) = 8.3\,\text{M}$ in triplicate, (B) control without poly(VBNOx) in triplicate. (C) Zeta potential of pristine PE, PE-poly(VBDMA) and PE-poly(VBNOx) at different pH. The pH was adjusted by titration with aqueous 0.05 M HCl. KCl was used as the supporting electrolyte, at a conductivity of 14 $\mu\text{S}\cdot\text{m}^{-1}$. Error bars represent standard deviations from measurements in both flow directions ($n = 2$) at each pH value. (D) Interaction of grafted polymeric *N*-oxides with acid fuchsin at pH = 3 for the determination of solvent-accessible positive charges.

(Figure S2, Table S1). However, it is difficult to derive precise estimates of the oxidation efficacy from these analyses.

To evaluate the impact of incomplete oxidation on surface properties, pH-dependent zeta potential measurements were conducted with PE-poly(VBDMA) and PE-poly(VBNOx). These measurements provide insight into the pH-dependent surface charge of these materials, which is critical for contact activity and thus potential antibacterial properties [35, 36]. The zeta potential of pristine PE, PE-poly(VBDMA), and PE-poly(VBNOx) was measured over a pH range of 3.9 to 9.4 (Figure 3C). The isoelectric points (IEPs) of the samples were determined as follows: PE at pH 5.4, PE-poly(VBDMA) at pH 7.8, and PE-poly(VBNOx) at pH 7.0. PE-poly(VBDMA) has a positive zeta potential at pH values below ~8. Antibacterial properties via a contact-active mechanism can therefore be expected for this material and have been confirmed by microbiological assays as shown later (Figure 5A). PE-poly(VBNOx) has a significantly lower zeta potential and is almost neutral at physiological pH, indicating that the oxidation step has converted most of the amino groups. This aligns well with the quantification of *N*-oxide and tertiary amino groups in the brush layers measured via adsorption of anionic dyes (Figure 3D). The colorimetric measurement was performed according to a literature procedure [27]. It revealed an oxidation efficacy of about 90% for PE-poly(VBNOx) (Figure S3). Given the low number of residual tertiary amines and the observed neutral surface zeta potential, an antibacterial effect of PE-poly(VBNOx) caused by contact activity is unlikely.

One of the most effective methods for the synthesis of poly(*N*-oxides) is the oxidation of tertiary amines with hydrogen peroxide. This post-grafting oxidation offers some notable benefits. It avoids the use of monomers with an *N*-oxide group for the graft-polymerization. These lead to charge repulsion and the formation of thinner and less homogeneous brush layers. In addition, the use of monomers with amine groups circumvents side reactions of *N*-oxide groups, such as heat-induced rearrangements in free radical polymerizations or deoxygenation, which can occur in Cu^0-mediated SI-ATRP protocols [37, 38]. Hydrogen peroxide is particularly attractive for post-grafting oxidation because it is cost-efficient and excess reagent can be easily decomposed into the non-toxic byproducts oxygen and water. However, hydrogen peroxide is known to bind strongly to *N*-oxides and it has been reported that excess hydrogen peroxide can be hard to remove from the reaction products [39]. The problem is particularly relevant for the synthesis of surface-bound polymer brushes. A large excess of hydrogen peroxide is typically used and *N*-oxide-bound hydrogen peroxide is hard to remove due to the limited solvent accessibility within the polymer brush layer. Generally, hydrogen peroxide can be eliminated either by quenching with reductive agents (e.g., thiosulfate, sulfite) or by accelerating its decomposition into oxygen and water using metals (e.g., MnO_2, Pt, Pd/C) [2]. However, the use of reductive agents for hydrogen peroxide quenching is not ideal because it can also lead to substantial reduction of *N*-oxide groups. Also, solid reagents like Pt or Pd/C cannot penetrate into the brush layer and are thus inefficient in quenching hydrogen peroxide. MnO_2 cannot be used either for the quenching of hydrogen peroxide, because polymeric *N*-oxides can form stable complexes with Mn(II) [40]. The cleanest, albeit time-consuming, method to remove hydrogen peroxide from brush layers is thus extensive

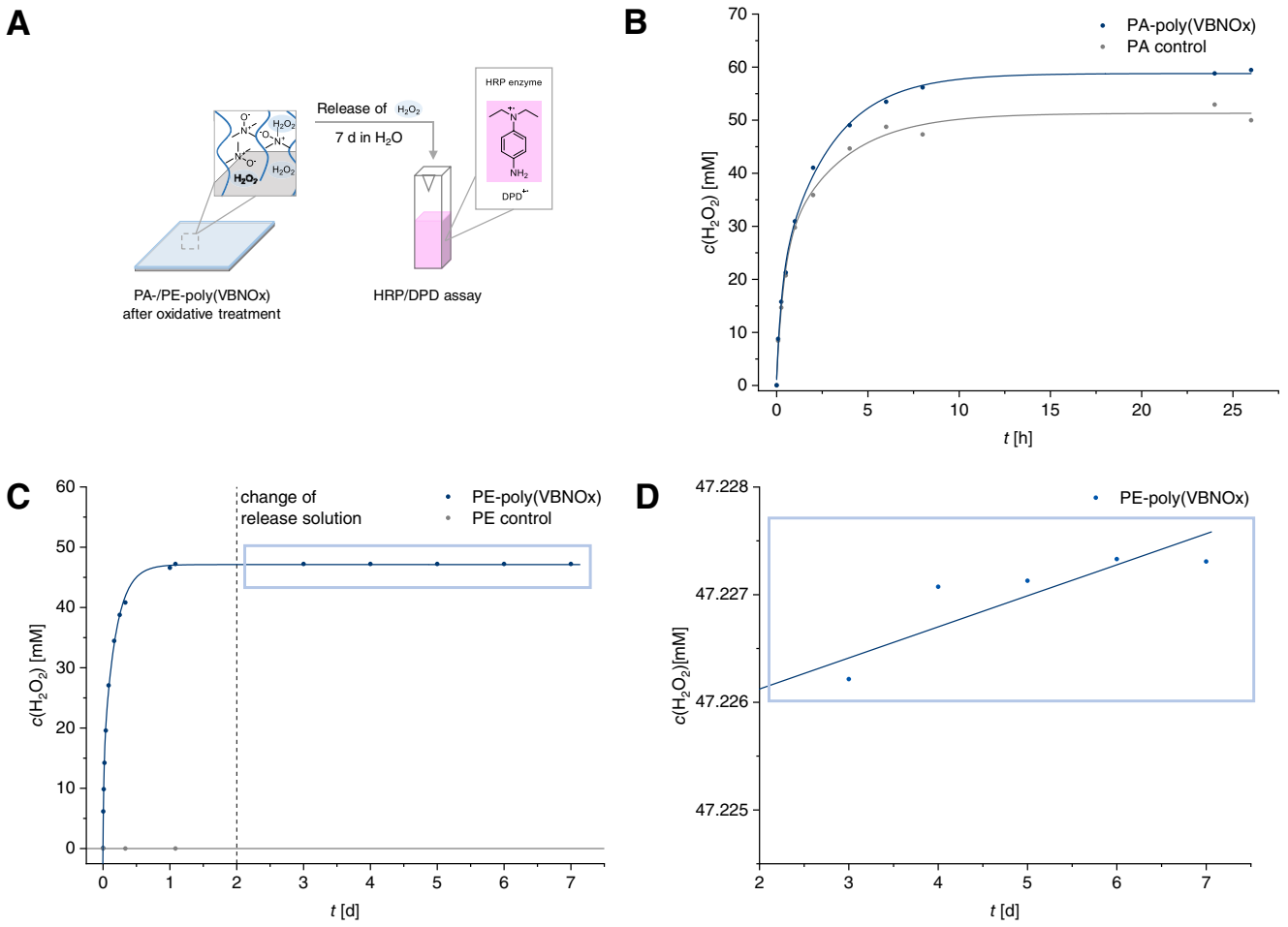

FIGURE 4 | (A) Release assay for the quantification of residual hydrogen peroxide from PE-poly(VBNOx) and PA-poly(VBNOx) prepared by the post-modification method. The release is measured by the oxidation of *N,N′*-diethyl-*p*-phenylenediamine (DPD) mediated by horseradish peroxidase (HRP). The formation of $DPD^{+\bullet}$ can be detected at 551 nm. (B) Release of hydrogen peroxide from polyamide 6 (PA, gray line) and PA-poly(VBNOx) (blue line) into water over 24 h. (C) Release of hydrogen peroxide from polyethylene (PE, gray line) and PE-poly(VBNOx) (blue line) into water over 7 days. The washing solution was changed after 48 h. (D) Enlarged figure of long-term release of hydrogen peroxide from PE-poly(VBNOx) into water from 2 to 7 days. The graph illustrates the continued, albeit slower, hydrogen peroxide release over time after the first large burst of peroxide release.

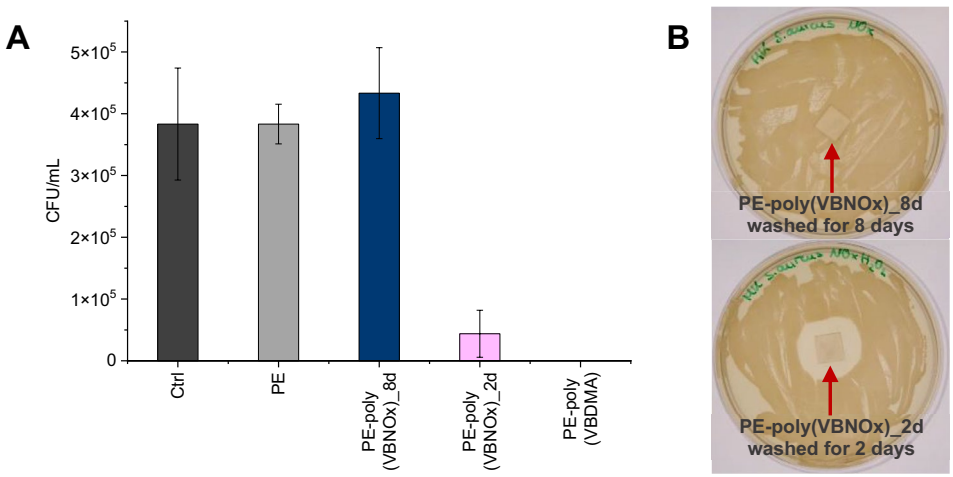

FIGURE 5 | (A) The antibacterial activities of hydrogen peroxide-free PE-poly(VBNOx)_8d, hydrogen peroxide-containing PE-poly(VBNOx)_2d and PE-poly(VBDMA) against *E. coli* (strain ATCC25922) were determined using a protocol adapted from ASTM E2149-13a. Colony counts were obtained after incubating the materials (1 cm^2) with bacterial suspensions (10^5 CFU·mL^{-1}) for 2 h and subsequent dilution (10^4–10^2 CFU·mL^{-1}) to determine the number of colony-forming units per milliliter (CFU/mL). Each experiment was performed in triplicate, with pristine PE as a control. Colony counts exceeding 200 were set as "too numerous to count". (B) Agar diffusion test DIN EN ISO 20645 of PE-poly(VBNOx)_8d and PE-poly(VBNOx)_2d with *S. aureus* (strain ATCC29213) after incubation for 20 h.

washing with water. Incomplete removal of hydrogen peroxide from brush layers might lead to misinterpretation of biological assays due to the delayed release of residual hydrogen peroxide into the solution. Hydrogen peroxide is a biocide [41] and its release might therefore lead to antibacterial properties that are not inherently due to the poly(*N*-oxide) material. To address this concern, the release of hydrogen peroxide from PE-poly(VBNOx) was studied with a sensitive assay involving the oxidation of *N,N′*-diethyl-*p*-phenylenediamine (DPD) mediated by horseradish peroxidase (HRP) and compared to equally hydrogen peroxide-treated pristine PE as a reference (Figure 4).

PE-poly(VBNOx) was prepared according to the method depicted in Figure 2, and the test specimens were washed three times with water under shaking for 10 s. The resulting samples of PE-poly(VBNOx) were suspended in 3 mL water for 48 h under shaking at room temperature. After 48 h, the test specimens were transferred to a fresh 3 mL of water to evaluate the long-term release over a further 5 days (Figure 4C). During the entire 7 days release period, 10 μL of the release solution was removed at each sampling time point. The amount of hydrogen peroxide released from the brush layer was quantified using the HRP/DPD assay. The spectrophotometric readout of the assay is based on the reaction of hydrogen peroxide with DPD in the presence of HRP, leading to the pinkish colored $DPD^{+\bullet}$, which can be quantified by measuring the UV absorbance at 551 nm (Figure S4) [42]. The assay reveals the slow release of large quantities of hydrogen peroxide from the PE-poly(VBNOx) test specimens, while equally treated PE shows no release after the hydrogen peroxide incubation and the brief washing process. Even after 2 days and the exchange of water, substantial amounts of hydrogen peroxide were released from the modified surface into the media.

After 2 h, a hydrogen peroxide concentration of 27 mM was detected in the release solution from 1 cm^2 of PE-poly(VBNOx) (Figure 4C). Two hours are also a typical incubation time for the evaluation of antibacterial properties of surfaces according to standard antimicrobial assays (e.g., ASTM E2149-13a) [43]. Considering the MIC of hydrogen peroxide for *S. aureus* (0.27–0.66 mM) and for *E. coli* (1.33–2.66 mM) [41], the concentration of released hydrogen peroxide exceeds the MICs by ~2 orders of magnitude. After prolonged washing, the total amount of hydrogen peroxide released from 1 cm^2 of PE-poly(VBNOx) corresponds to approximately 140 μmol, based on a maximum detected concentration of 47 mM in 3 mL water. The amount of accessible *N*-oxide groups on these test specimens is about 17 $nmol \cdot cm^{-2}$ as determined via the colorimetric assay mentioned above (Figure 3D). This number underestimates most likely the number of *N*-oxides accessible for hydrogen peroxide (because the dye used is significantly larger then hydrogen peroxide). However, it suggests that each *N*-oxide group can bind several molecules hydrogen peroxide in the brush layer. It is notable that after washing with fresh water for periods longer than 48 h low, but still significant amounts of hydrogen peroxide were released, which still exceed the MIC for *S. aureus* (Figure 4D).

For the evaluation of the impact of the base material on hydrogen peroxide adsorption, PA-poly(VBNOx) test specimens were prepared by the same grafting method and analyzed with IR, goniometry, and a fluorescein dye assay (Figure S5, Table S1). Hydrogen peroxide-treated PA and PA-poly(VBNOx) were then suspended in 3 mL water for 24 h (Figure 4B). PA-poly(VBNOx) gave similar results compared to PE-poly(VBNOx), with a final release concentration of hydrogen peroxide of 59 mM after 24 h. In contrast to PE, however, the use of PA also leads to significant adsorption of hydrogen peroxide into the more polar unmodified base material. The capacity of poly(*N*-oxide) brush layers to bind and gradually release hydrogen peroxide over several days might thus be a plausible explanation for previously observed antimicrobial activities or redox activities of these materials [23, 24, 32].

The antibacterial properties of *N*-oxide brush polymers were evaluated by testing PE-poly(VBNOx) test specimens submitted to washing with water for 2 (PE-poly(VBNOx)_2d) and 8 days (PE-poly(VBNOx)_8d). Pristine PE was used as a negative control and PE-poly(VBDMA) as a polycationic and thus contact-active material. The stability of PE-poly(VBDMA) and PE-poly(VBNOx) against prolonged treatment with water was demonstrated in previous studies and has been confirmed here for each sample via IR spectroscopy and goniometry (Figure S6). Gram-negative *E. coli* (ATCC25922) was used as a test microorganism following ASTM E2149-13a (Figure 5A). Sterilized material samples (size of 1 cm^2) were incubated with bacterial suspensions (10^5 $CFU \cdot mL^{-1}$ in saline) at 37°C for 2 h. After incubation, the suspensions were serially diluted (10^4–10^2 $CFU \cdot mL^{-1}$) and plated onto Columbia agar for colony counting after 17 h of incubation at 37°C.

The assay confirmed the contact-activity of PE-poly(VBDMA), which led to complete elimination of bacteria. PE-poly(VBNOx)_8d had no antibacterial activity against *E. coli* leading to colony counts comparable to the growth control (Ctrl) and PE. In contrast, PE-poly(VBNOx)_2d had a significant yet lower antibacterial activity than PE-poly(VBDMA). The antibacterial activity of PE-poly(VBNOx)_2d can be attributed to hydrogen peroxide release from the *N*-oxide-brush layer. The biocide release was confirmed with an agar diffusion test (DIN EN ISO 20645). While PE-poly(VBNOx)_8d showed no inhibition zone, the hydrogen peroxide-releasing PE-poly(VBNOx)_2d led to a clear inhibition zone (Figure 5B). These findings indicate that the observed antibacterial effects are due to a contact-active mechanism for PE-poly(VBDMA) and a release of residual amounts of hydrogen peroxide from PE-poly(VBNOx)_2d.

Complete removal of residual hydrogen peroxide is thus essential for accurate evaluation of the intrinsic antibacterial properties of poly(*N*-oxide)-modified surfaces. On the other hand, the observed ability of polymeric *N*-oxides for uptake and gradual release of hydrogen peroxide over several days is also a feature of these materials for biomedical applications. Polymeric alkylamine *N*-oxide modified surfaces naturally possess low-fouling properties, reduce bacterial adhesion and biofilm formation [8]. However, they usually lack inherent antibacterial activity. By utilizing the reversible binding and release of hydrogen peroxide, these surfaces can be temporarily activated for disinfection, effectively combining antibacterial action with their low-fouling characteristics for enhanced functionality in critical environments.

3 | Conclusion

Poly(*N*-oxides) have excellent blood compatibility, are non-immunogenic, and have antifouling properties due to high surface hydration. Many biomedical applications of these materials are based on the assumption that the *N*-oxide groups are unreactive and biologically inert. However, several *N*-oxides of low molecular weight have rather high chemical reactivity. Also, for polymeric *N*-oxides, both stealth effects and antimicrobial activity have been described. Given the inconclusive results on the bioactivity of polymeric *N*-oxides in previous studies, this work explores the antibacterial and stealth properties of PE-poly(VBNOx) and similar derivatives. No formation of reactive radical species was observed by EPR-spectroscopy and a colorimetric assay with DPBF. The redox reactivity of the polymeric *N*-oxides tested does therefore not lead to antibacterial properties of the material. This study focuses on PE-poly(VBNOx) and similar derivatives, but the same chemical inertness can also be expected for many other polymeric *N*-oxides with alkylamine *N*-oxide groups. In addition, an evaluation of the surface zeta potential revealed that PE-poly(VBNOx) has a neutral surface potential at physiological pH. A contact-active antibacterial mechanism of polymeric *N*-oxides is thus also unlikely.

Polymeric *N*-oxides have therefore no intrinsic antibacterial properties against planktonic bacteria. Instead, the antibacterial effect observed with these materials in our own previous studies and those of other authors was most likely caused by the release of hydrogen peroxide, a direct consequence of a commonly employed synthetic protocol using post-polymerization oxidation of tertiary amines to *N*-oxides using hydrogen peroxide. Excess hydrogen peroxide is bound strongly to *N*-oxide groups and thus hard to remove from polymeric *N*-oxides. This leads to a delayed release of hydrogen peroxide into water over several days, effectively eliminating bacteria such as *S. aureus* and *E. coli*.

This study has limitations because it addresses the activity of PE-poly(VBNOx) against planktonic cultures of bacteria only. The protonation of *N*-oxide groups in more acidic environments found in biofilms [44] might lead to antibacterial properties caused by contact activity.

The delayed hydrogen peroxide release of polymeric *N*-oxides does not only compromise microbiological assays but is also a functional feature for some biomedical applications. However, it must be carefully considered when evaluating the inherent bioactivity (antibacterial or cytotoxicity) of poly(*N*-oxide)-modified surfaces. Neglecting the presence of residual hydrogen peroxide may result in an inaccurate assessment of the intrinsic antibacterial properties or the redox reactivity of these materials. However, it should be noted that the release of hydrogen peroxide from polymeric *N*-oxides depends on the material investigated. For water-soluble polymers it is expected to be significantly faster than from grafted polymers on solid supports. Furthermore, factors such as chain length and the degree of cross-linking could have an influence.

For applications where inert properties of poly(*N*-oxides) are required (e.g., polymers for drug delivery) [9], the complete removal of residual hydrogen peroxide is essential. This can be achieved by thorough washing with water over several days. The absence of hydrogen peroxide should be confirmed via hydrogen peroxide test strips.

Overall, this study highlights the dual nature of poly(*N*-oxide)-modified surfaces: as materials capable of controlled antibacterial action through hydrogen peroxide uptake and release and as inert low-fouling materials when properly purified. These findings provide valuable guidance for the design and evaluation of poly(*N*-oxide)-based materials in pharmaceutical, biomedical, and polymer applications.

4 | Experimental Section

4.1 | Chemicals and Materials

PE foils (0.75 mm thickness) were purchased from Goodfellow and PA foils (0.50 mm thickness) from Reichelt Chemietechnik GmbH + Co. Acid fuchsin disodium salt, azobisisobutyronitrile (AIBN, 98%), cetyltrimethylammonium chloride (CTAC) (96%), dimethylamine solution (33 vol% in EtOH), DMPO, aqueous hydrogen peroxide solution (30 vol%), HRP (> 250 units/mg solid), NaH_2PO_4, Na_2HPO_4, and 4-vinylbenzyl chloride (90%) were obtained from Sigma-Aldrich. DPBF and fluorescein disodium salt were purchased from Thermo Fisher Scientific, and DPD sulfate was acquired from BLDpharm. VBDMA [45], poly(VBDMA) [27] and poly(VBNOx) [27] were prepared according to literature procedures. All reagents were used without further purification. *S. aureus* (strain ATCC29213) and *E. coli* (strain ATCC29522) were obtained from American Type Culture Collection.

4.2 | Contact Angle Measurement

Contact angle measurements were performed using an OCA 20 goniometer (DataPhysics, Filderstadt, Germany) equipped with dual automated dispensing units, a high-speed CCD camera system, a motorized stage, and halogen lighting for static and dynamic analyses. Advancing contact angles were determined using the static sessile drop method with deionized water ($V = 5\,\mu L$). Contact angles were calculated using the instrument's integrated OCA software.

4.3 | NMR Spectroscopy

The measurements were conducted in 5 mm outer diameter sample tubes using a Bruker Avance III HD 400 MHz NMR spectrometer (AV400, Bruker, Ettlingen, Germany). The resulting ^{1}H-NMR spectra were processed using MestReNova x64 software, with the signals referenced to the solvent signal of MeOD.

4.4 | IR Spectroscopy

IR spectra were recorded using an attenuated total reflectance Fourier Transform IR system (ATR-FTIR), model IRAffinity-1S

from Shimadzu (Kyoto, Japan), equipped with a "Quest" ATR accessory from Specac (London, England). The spectral range was set from 4000 to 450 cm^{-1}, with a resolution of 0.5 cm^{-1} in absorbance mode. The obtained spectra were processed with OriginPro 10 (2025) software.

4.5 | EPR Spectroscopy

EPR spectroscopy was conducted using a Magnettech Miniscope MS400 X-band benchtop spectrometer (9.30–9.55 GHz). Samples were measured in 4 mm quartz glass EPR tubes at 77 K after incubation of poly(VBNOx) (6.3 mg) with DMPO (100 mM in MeOH) as a spin trap to detect short-lived radicals at 37°C. Data analysis was performed using ESR-MPlot and Analyze software.

4.6 | Zeta Potential Measurements

Zeta potential measurements of pristine PE, PE-poly(VBDMA), and PE-poly(VBNOx) were conducted using a SurPASS 1 electrokinetic analyzer (Anton Paar, Graz, Austria) in an adjustable gap cell, where two rectangular samples (1 cm × 2 cm) were positioned opposite each other with a 100–120 μm distance. The starting conductivity was set to 14–17 $\mu S \cdot m^{-1}$ using KCl as the supporting electrolyte. The pH was gradually adjusted from 9.4 to 3.9 through titration with 0.05 M HCl in a KOH solution. To ensure accurate measurements and prevent interference from dissolved gasses, the solution was degassed by purging with N_2 throughout the entire setup and measurement process. The zeta potential was calculated from the streaming potential using the Helmholtz–Smoluchowski equation.

4.7 | X-Ray Photoelectron Spectroscopy (XPS)

XPS measurements were carried out using a KRATOS AXIS Ultra DLD system (Kratos Analytical, Manchester, UK) equipped with a monochromatic Al Kα source operating at 15 kV and 225 W. Survey spectra were acquired with a pass energy of 160 eV, while high-resolution region spectra were recorded at 20 eV. The analysis area was 700 × 300 μm^2. Charge neutralization was applied to all PE-based samples to compensate for surface charging. Data evaluation and validation were performed using CASA-XPS software (version 2.3.24). Spectra were calibrated by setting the C1s peak to 284.5 eV. Prior to deconvolution, background subtraction (using either Shirley or U2 Tougaard methods) was applied to the region spectra.

4.8 | Time-of-Flight Secondary Ion Mass Spectrometry (ToF-SIMS) and Scanning Probe Microscopy (SPM)

Analyses were performed using an M6 Plus instrument (IONTOF GmbH, Münster, Germany), equipped with an integrated scanning probe microscope (SPM) inside the main vacuum chamber, enabling direct correlation of topographic and mass spectrometric data.

ToF-SIMS measurements employed 60 keV Bi_3^{2+} primary ions (I = 0.05 pA, 200 μs cycle time) using the Nanoprobe 50 in high-current bunched mode with a 700 μm beam-defining aperture. Depth profiling was conducted in non-interlaced mode using a 5 keV Ar_{2000}^{+} sputter beam (I = 1.328 nA). Charge compensation was achieved with low-energy electrons during a 1 s pause between cycles.

The analysis area was 70 × 70 μm^2 (128 × 128 pixels), centered within a 200 × 200 μm^2 sputter crater. Profiling was terminated at the interface between the coating and the substrate. SPM images of the analysis area were recorded before and after SIMS measurements in intermittent mode at 2048 × 128 pixel resolution, along with x and y line scans (600 μm length each).

Data were evaluated using SurfaceLab 7.3 (IONTOF GmbH). Negative ion mode spectra were acquired, achieving a mass resolution of $m/\Delta m > 7500$ (FWHM) at $m/z = 65.04$ ($C_5H_5^-$).

4.9 | Preparation of Poly(VBDMA) Brushes on PE (PE-Poly(VBDMA)) and PA (PA-Poly(VBDMA))

The polymerization was performed using an adapted protocol from Burmeister et al. [23].

PE foils (1 cm^2, 0.75 mm thickness) and PA foils (1 cm^2, 0.50 mm thickness) were cleaned by ultrasonication in EtOH (5 mL) for 10 min, followed by drying at 50°C prior to use.

Plasma activation was carried out using an atmospheric air plasma system from Plasmatreat GmbH (Steinhagen, Germany). The non-equilibrium plasma discharge was generated at atmospheric pressure using a FG5001 generator operating at a working frequency of 21 kHz. Plasma treatment was applied via a rotating jet nozzle (RD1004) equipped with a stainless-steel tip (No. 22826), providing an expanded treatment width of approximately 22 mm. Plasma treatment of the foils was performed at a distance of 6 mm between the plasma jet nozzle and the surface. The speed of the plasma jet nozzle was set at 110 $mm \cdot s^{-1}$. After plasma exposure, samples were stored under ambient conditions for 8 min before further processing.

A solution of VBDMA (1.00 g, 50 wt%) and AIBN (25 mg) in EtOAc was degassed by Ar-purging for 10 min. Plasma-activated foils were then added to the solution, followed by an additional 15 min of Ar-purging. Polymerization was carried out at 80°C for 4 h. After the reaction, the foils were washed twice with EtOAc (5 mL) and once with EtOH (5 mL), each for 10 min using ultrasonication, and then dried at room temperature.

4.10 | Preparation of Poly(VBNOx) Brushes on PE (PE-Poly(VBNOx)) and PA (PA-Poly(VBNOx))

Poly(VBDMA) brushes grafted from PE (PE-poly(VBDMA)) and PA (PA-poly(VBDMA)) were oxidized by shaking in hydrogen peroxide (30 wt%, 3 mL) for 3 days. For complete removal of hydrogen peroxide, the foils were briefly washed with water (3

×2 mL, 10 s shaking per wash cycle), followed by extended shaking in water (3 mL) for 8 days.

4.11 | DPBF Assay

DPBF (2.7 mg) was dissolved in EtOH (10 mL) and subsequently diluted to $c = 0.041$ mg/mL with EtOH. Poly(VBNOx) (6 mg) was dissolved in MeOH (2 mL). For the control samples ($n = 3$), MeOH (0.6 mL) was mixed with DPBF solution (0.6 mL, $n(\text{DPBF})_{\text{start}} = 0.090$ μmol). In parallel, test samples ($n = 3$) were prepared by adding DPBF solution (0.6 mL) to the poly(VBDMA) solution (0.6 mL, $n(N\text{-oxide}) = 10$ mmol). All samples were incubated at 37°C and kept in the dark throughout the experiment. UV–vis spectra were recorded in the range of 350–550 nm at $t = 0$ min and $t = 24$ h.

4.12 | Hydrogen Peroxide Release Assay

Poly(VBNOx)-modified surfaces (1 cm^2) were briefly rinsed with water (3 ×2 mL; 10 s of shaking per wash cycle) following preparation with hydrogen peroxide. The surfaces were then incubated in water (3 mL) at room temperature under shaking at 500 rpm for 48 h. Aliquots (10 μL) were collected at the following time points: $t = 0$ min, 5 min, 15 min, 30 min, 1 h, 2 h, 4 h, 6 h, 8 h, 24 h, and 26 h.

After the initial 48 h period, the surfaces were transferred to fresh water (3 mL) and incubated under the same conditions (500 rpm, room temperature) for an additional 5 days. Prior to analysis, all collected samples were appropriately diluted to ensure hydrogen peroxide concentrations fell within the linear detection range (0.78–25 μM) of the DPD assay.

4.13 | DPD Assay

DPD (10 mg) was dissolved in water (0.9 mL) and 1 M H_2SO_4 (0.1 mL) to prepare the DPD stock solution. HRP (1 mg) was dissolved in water (1 mL) to prepare the HRP stock solution. The PBS buffer was prepared by mixing an aqueous solution of Na_2HPO_4 (1 M, 10 mL) and an aqueous solution of NaH_2PO_4 (1 M, 90 mL). For each DPD assay, a reaction mixture was prepared by combining water (3 mL), PBS buffer (0.3 mL), DPD solution (30 μL), HRP solution (30 μL), and hydrogen peroxide sample solution (30 μL). The mixture was shaken for 2 min prior to measuring the UV–vis absorption at 551 nm. A calibration curve was generated using hydrogen peroxide concentrations ranging from 0.78 to 25 μM.

4.14 | Acid Fuchsin Dye Assay

The dye assay was performed using a modified literature protocol [27]. PE-poly(VBNOx) (1 cm^2) was treated with acid fuchsin solution (1.0 wt%, 2 mL, pH = 3) under shaking at 100 rpm for 30 min at room temperature. To remove residual dye, the foils were subsequently immersed in aqueous HCl solution (pH = 3) for 10 min. For dye desorption, the foils were treated with aqueous CTAC solution (0.1 wt%, 5 mL) and shaken at 100 rpm for 1 h. After desorption, the pH of the solution was adjusted to pH = 3 using 1 M aqueous HCl, and the UV–vis absorption was measured at 556 nm. The absorbance of a solution obtained from a pristine PE foil, processed in the same manner, was subtracted as the blank value. The concentration of solvent-accessible *N*-oxides was calculated using the extinction coefficient (ε) of acid fuchsin in CTAC of 38,125 $M^{-1} \cdot cm^{-1}$.

4.15 | Fluorescein Dye Assay

The dye assay was performed using a modified literature protocol [46]. PA-poly(VBNOx) (1 cm^2) foils were incubated in 5 mL of a 1 wt% fluorescein solution at room temperature for 30 min under gentle shaking. After staining, the foils were rinsed with water and further cleaned in 10 mL of water for 10 min. Dye desorption was carried out by immersing the stained foils in 5 mL of a 0.1 wt% CTAC solution (1:9 PBS buffer pH = 8 and water) for 30 min under shaking. The desorbed dye was quantified by UV–vis spectroscopy at 501 nm using an extinction coefficient of 77,000 $L \cdot mol^{-1} \cdot cm^{-1}$. The absorbance of a solution obtained from a pristine PA foil, processed in the same manner, was subtracted as the blank value.

4.16 | Determination of Antibacterial Activity ASTM E2149-13a

The antimicrobial activity of the modified samples was evaluated following a procedure adapted from ASTM assay E2149-13a [43]. All test samples were sterilized with ^{i}PrOH and then dried under laminar airflow prior to testing. Bacterial strains *S. aureus* (ATCC29213) and *E. coli* (ATCC25922) were cultured overnight on Columbia agar. The overnight cultures were harvested, suspended, and diluted in sterile saline solution (0.9%) to maintain a cell density of 1.5×10^8 cells/mL (OD = 0.5), and further diluted to a final concentration of 10^5 colony-forming units per milliliter (CFU/mL). PE surfaces (1 cm^2) were placed in sterile tubes and covered with 2.0 mL of the respective bacterial suspension (10^5 CFU/mL). The samples were incubated at 37°C for 2 h in ambient air. After incubation, the solutions, along with three subsequent dilutions (100 μL of 10^5, 10^4, 10^3, and 10^2 CFU/mL), were cultured on Columbia agar plates and incubated at 37°C for 17 h. Colony counts were then performed to determine the number of colony-forming units per milliliter (CFU/mL), with values above 200 CFU considered "too numerous to count." Each experiment was conducted in triplicate.

4.17 | Agar Diffusion Plate Test DIN EN ISO 20645

The leaching of antibacterial components from PE-poly(VBNOx) was evaluated using the agar diffusion assay in accordance with DIN EN ISO 20645:2002-02. Briefly, a Columbia agar plate was inoculated with 200 μL of bacterial suspension containing *S. aureus* (ATCC29213) at a concentration of 1.5×10^8 CFU/mL. Test specimens (1 cm^2) were placed with the modified surface onto the inoculated agar plate and incubated at 37°C for 20 h. After incubation, the plates were examined for the presence of

an inhibition zone surrounding the samples, indicating antibacterial activity.

Acknowledgments

We thank Antje Wagner for proofreading of the manuscript. We acknowledge financial support from the Open Access Publication Fund of Universität Hamburg. EPR-measurements were supported by Thomas Marx and Peter Burger. XPS was measured by Nico Scharnagl, ToF-SIMS was measured by Marcus Rohnke. This project has received funding from the Federal Ministry for Economic Affairs and Climate Action under the programme ZIM (Zentrales Innovationsprogramm Mittelstand) under grant agreement No KK5559001IE3.

References

1. T. Yang, D. M. Andrada, and G. Frenking, "Dativeversuselectron-Sharing Bonding in N-Oxides and Phosphane Oxides R3EO and Relative Energies of the R2EOR Isomers (E = *N*, P; *R* = H, F, cl, Me, Ph). A Theoretical Study," *Physical Chemistry Chemical Physics* 20 (2018): 11856–11866.

2. M. Kobus, T. Friedrich, E. Zorn, N. Burmeister, and W. Maison, "Medicinal Chemistry of Drugs With N-Oxide Functionalities," *Journal of Medicinal Chemistry* 67 (2024): 5168–5184.

3. T. Friedrich, M. Kobus, S. Mesgarha, E. Moretto, L. Grosche, and W. Maison, "Tailoring the Properties of Functional Materials With N-Oxides," *Advanced Functional Materials* (2025): e15786, https://doi.org/10.1002/adfm.202515786.

4. P. Sarker, T. Lu, D. Liu, et al., "Hydration Behaviors of Nonfouling Zwitterionic Materials," *Chemical Science* 14 (2023): 7500.

5. H. Huang, C. Zhang, R. Crisci, et al., "Strong Surface Hydration and Salt Resistant Mechanism of a New Nonfouling Zwitterionic Polymer Based on Protein Stabilizer TMAO," *Journal of the American Chemical Society* 143 (2021): 16786.

6. Z. Feng, X. Feng, and X. Lu, "BioinspiredN-Oxide-Based Zwitterionic Polymer Brushes for Robust Fouling-Resistant Surfaces," *Environmental Science & Technology* 57 (2023): 7298.

7. V. S. Luc, C. C. Lin, S. Y. Wang, et al., "Antifouling Properties of Amine-Oxide-Containing Zwitterionic Polymers," *Biomacromolecules* 24 (2023): 5467.

8. B. Li, P. Jain, J. Ma, et al., "TrimethylamineN-Oxide–Derived Zwitterionic Polymers: A New Class of Ultralow Fouling Bioinspired Materials," *Science Advances* 5 (2019): eaaw9562.

9. W. Fan, Q. Wei, J. Xiang, et al., "Mucus Penetrating and Cell-Binding Polyzwitterionic Micelles as Potent Oral Nanomedicine for Cancer Drug Delivery," *Advanced Materials* 34 (2022): 2109189.

10. C. D. G. Read, P. W. Moore, and C. M. Williams, "N,N,N′,N′-Tetramethylenediamine Dioxide (TMEDAO2) Facilitates Atom Economical/Open Atmosphere Ley–Griffith (TPAP) Tandem Oxidation-Wittig Reactions," *Green Chemistry* 17 (2015): 4537–4540.

11. A. M. Mfuh and O. V. Larionov, "Heterocyclic N-Oxides – An Emerging Class of Therapeutic Agents," *Current Medicinal Chemistry* 22 (2015): 2819–2857.

12. H. Cerecetto and M. González, "N-Oxides as Hypoxia Selective Cytotoxins," *Mini-Reviews in Medicinal Chemistry* 1 (2001): 219–231.

13. G. Rivera, "Quinoxaline 1,4-di-N-Oxide Derivatives: Are They Unselective or Selective Inhibitors?," *Mini Reviews in Medicinal Chemistry* 22 (2022): 15–25.

14. S. Leyva-Ramos and A. Pedraza-Alvarez, "Quinoxaline 1,4-di-N-Oxides: A Review of the Importance of Their Structure in the Development of Drugs Against Infectious Diseases and Cancer," *Medicinal Chemistry Research* 30 (2021): 1175–1184.

15. L. H. Patterson and S. R. McKeown, "AQ4N: A New Approach to Hypoxia-Activated Cancer Chemotherapy, 1593," *British Journal of Cancer* 83 (2000): 1589–1593.

16. S. Fraud, J. Y. Maillard, M. A. Kaminski, and G. W. Hanlon, "Activity of Amine Oxide Against Biofilms of *Streptococcus mutans*: A Potential Biocide for Oral Care Formulations," *Journal of Antimicrobial Chemotherapy* 56 (2005): 672–677.

17. D. Kang, S. T. Cheung, A. Wong-Rolle, and J. Kim, "EnamineN-Oxides: Synthesis and Application to Hypoxia-Responsive Prodrugs and Imaging Agents," *ACS Central Science* 7 (2021): 631–640.

18. Z. Ding, Z. Guo, Y. Zheng, Z. Wang, Q. Fu, and Z. Liu, "Radiotherapy ReducesN-Oxides for Prodrug Activation in Tumors," *Journal of the American Chemical Society* 144 (2022): 9458–9464.

19. S. E. Walsh, J. Y. Maillard, A. D. Russell, C. E. Catrenich, D. L. Charbonneau, and R. G. Bartolo, "Activity and Mechanisms of Action of Selected Biocidal Agents on Gram-Positive and -Negative Bacteria," *Journal of Applied Microbiology* 94 (2003): 240–247.

20. C. R. Birnie, D. Malamud, and R. L. Schnaare, "Antimicrobial Evaluation ofN-Alkyl Betaines andN-Alkyl-N,N-Dimethylamine Oxides With Variations in Chain Length," *Antimicrobial Agents and Chemotherapy* 44 (2000): 2514–2517.

21. F. Devínsky, A. Kopecka-Leitmanová, F. Šeršeň, and P. Balgavý, "Cut-Off Effect in Antimicrobial Activity and in Membrane Perturbation Efficiency of the Homologous Series ofN,N-Dimethylalkylamine Oxides," *Journal of Pharmacy and Pharmacology* 42 (1990): 790–794.

22. Q. Xin, Z. Ma, S. Sun, et al., "Supramolecular Self-Healing Antifouling Coating for Dental Materials," *ACS Applied Materials and Interfaces* 15 (2023): 41403–41416.

23. N. Burmeister, E. Zorn, A. Farooq, et al., "Surface GraftedN-Oxides Have Low-Fouling and Antibacterial Properties," *Advanced Materials Interfaces* 10 (2023): 2300505.

24. N. Zhang, K. Cheng, J. Zhang, N. Li, X. Yang, and Z. Wang, "A Dual-Biomimetic Strategy to Construct Zwitterionic Anti-Fouling Membrane With Superior Emulsion Separation Performance," *Journal of Membrane Science* 660 (2022): 120829.

25. W. D. Loecker and G. Smets, "Hydrolysis of Methacrylic Acid–Methyl Methacrylate Copolymers," *Journal of Polymer Science* 40 (2003): 203–216.

26. D. M. Yourtee, R. E. Smith, K. A. Russo, et al., "The Stability of Methacrylate Biomaterials When Enzyme Challenged: Kinetic and Systematic Evaluations," *Journal of Biomedical Materials Research* 57 (2001): 522–531.

27. E. Moretto, M. Kobus, and W. Maison, "Interaction of Grafted PolymericN-Oxides With Charged Dyes," *Langmuir* 41 (2025): 11136–11146.

28. X. Shen and K. S. Gates, "Enzyme-Activated Generation of Reactive Oxygen Species From HeterocyclicN-Oxides Under Aerobic and Anaerobic Conditions and Its Relevance to Hypoxia-Selective Prodrugs," *Chemical Research in Toxicology* 32 (2019): 348–361.

29. T. Entradas, S. Waldron, and M. Volk, "The Detection Sensitivity of Commonly Used Singlet Oxygen Probes in Aqueous Environments," *Journal of Photochemistry and Photobiology. B* 204 (2020): 111787.

30. M. J. Davies, "Detection and Characterisation of Radicals Using Electron Paramagnetic Resonance (EPR) Spin Trapping and Related Methods," *Methods* 109 (2016): 21–30.

31. F. Pan, C. Sun, Y. Li, et al., "Solution-Processable n-Doped Graphene-Containing Cathode Interfacial Materials for High-Performance Organic Solar Cells," *Energy and Environmental Science* 12 (2019): 3400–3411.

32. M. Lv, Y. Li, X. Wei, Y. Xu, Z. Ge, and X. Chen, "Intermolecular n-Doping Nonconjugated Polymer Cathode Interfacial Materials for Organic Solar Cells," *ACS Applied Energy Materials* 2 (2019): 2238–2245.

33. D. A. Dobrzanska, A. L. Cooper, C. G. Dowson, et al., "Oxidation of Tertiary Amine-Derivatized Surfaces to Control Protein Adhesion," *Langmuir* 29 (2013): 2961–2970.

34. I. Lee, J. Roh, J. Lee, J. Song, and J. Jang, "Antibacterial Performance of Various Amine Functional Polymers Coated Silica Nanoparticles," *Polymer* 83 (2016): 223–229.

35. O. Rzhepishevska, S. Hakobyan, R. Ruhal, J. Gautrot, D. Barbero, and M. Ramstedt, "The Surface Charge of Anti-Bacterial Coatings Alters Motility and Biofilm Architecture," *Biomaterials Science* 1 (2013): 589–602.

36. N. Burmeister, E. Zorn, L. Preuss, et al., "Low-Fouling and Antibacterial Polymer Brushes via Surface-Initiated Polymerization of a Mixed Zwitterionic and Cationic Monomer," *Langmuir* 39 (2023): 17959–17971.

37. S. K. Singh, M. Srinivasa Reddy, M. Mangle, and K. Ravi Ganesh, "Cu(I)-Mediated deoxygenation of N-oxides to amines," *Tetrahedron* 63 (2007): 126–130.

38. E. Zorn, J. I. H. Knaack, N. Burmeister, et al., "Contact-Biocide TiO-2Surfaces by Surface-Initiated Atom Transfer Radical Polymerization With Chemically Stable Phosphonate Initiators," *Langmuir* 39 (2023): 11063–11072.

39. B. Xing, X. Liu, Y. Wang, et al., "Catalytic Decomposition of Residual Hydrogen Peroxide in N-Methylmorpholine-N-Oxide by Heteroatom doping Modified Activated Carbon," *Materials Today Communications* 41 (2024): 110350.

40. L. C. Nathan and R. O. Ragsdale, "Chromium(III), manganese(II), iron(III), and Zinc(II) Complexes of Some Substituted Aromatic Amine n-Oxides," *Inorganica Chimica Acta* 3 (1969): 473–477.

41. Y. S. Raval, L. Flurin, A. Mohamed, K. E. Greenwood-Quaintance, H. Beyenal, and R. Patel, "In VitroAntibacterial Activity of Hydrogen Peroxide and Hypochlorous Acid, Including That Generated by Electrochemical Scaffolds," *Antimicrobial Agents and Chemotherapy* 65 (2021): 65.

42. L. Shi, L. Yang, W. Zhou, et al., "Photoassisted Construction of Holey Defective g-C3N4Photocatalysts for Efficient Visible-Light-Driven H_2O_2 Production," *Small* 14 (2018): 14.

43. M. van de Lagemaat, A. Grotenhuis, B. van de Belt-Gritter, et al., "Comparison of Methods to Evaluate Bacterial Contact-Killing Materials," *Acta Biomaterialia* 59 (2017): 139–147.

44. S. B. Behbahani, S. D. Kiridena, U. N. Wijayaratna, C. Taylor, J. N. Anker, and T. J. Tzeng, "pH Variation in Medical Implant Biofilms: Causes, Measurements, and Its Implications for Antibiotic Resistance," *Frontiers in Microbiology* 13 (2022): 1028560.

45. N. Burmeister, C. Vollstedt, C. Kroger, et al., "Zwitterionic Surface Modification of Polyethylene via Atmospheric Plasma-Induced Polymerization of (Vinylbenzyl-)sulfobetaine and Evaluation of Antifouling Properties," *Colloids and Surfaces B: Biointerfaces* 224 (2023): 113195.

46. S. Kliewer, S. G. Wicha, A. Broker, et al., "Contact-Active Antibacterial Polyethylene Foils via Atmospheric Air Plasma Induced Polymerisation of Quaternary Ammonium Salts," *Colloids and Surfaces B: Biointerfaces* 186 (2020): 110679.

Supporting Information

Additional supporting information can be found online in the Supporting Information section. **Data S1:** Supporting Information.